S1 Sensitivity of WMTE detection to parameter choices

The WMTE detection algorithm has three free parameters: the magnitude threshold, the direction filter applied to each grid point, and the minimum size of detected objects. To make appropriate choice of parameter values and understand the impact of parameter choice on the model, we ran the WMTE detection algorithm with different combinations of these parameters. We varied the magnitude threshold from 60% to the atmospheric river threshold of 85% from Guan and Waliser, 2015, upon which our method is based, the direction threshold by 10% around 45°, and the size threshold from 750 to 1000 pixels. We ran the detector with all combinations of these parameters, resulting in a total of 36 runs. The parameter values tested are shown in table S1.

Table S1: The parameter values used in the sensitivity analysis

Magnitude threshold	60, 70, 80, 85
Direction threshold	40.5, 45, 49.5
Minimum size	750, 1000, 1500

To study the impact of parameter choice on EEA westerlies, we compare the statistics of events crossing the EEA line (29°E, 2°N to 12°S) for the different combinations. The percentage change in basic statistics when we change the parameter values from magnitude threshold=70%, direction threshold=45°, size threshold=1000 are shown in Fig. S1. On each plot, the colour of the line represents the minimum size, and the line style represents the direction, so that following a single line shows the effect of changing the magnitude threshold for constant direction and size.

Fig. S1a shows the effect of parameter choice on the number of WMTE days per month crossing the EEA line. For all combinations of the other parameters, the number of days decreases as the magnitude threshold increases, as would be expected. The decrease is roughly linear, but the rate increases for thresholds above 70%. The number of days per month increases with increasing values of the direction filter and with decreasing values of the size filter, but the lines are all relatively close together, showing that there is less sensitivity to these parameters.

We also show the statistics of 'events': periods of consecutive days where there was a WMTE crossing the EEA line. Fig. S1b shows the average number of events per month, which shows similar patterns to those in the number of days per month, but the gradient is more constant and only steepens above a threshold of 80%. Fig. S1c shows the mean length of events. The lines in this plot are more clustered and have a shallower gradient, showing that mean duration was less sensitive to parameter change. For all configurations, the gradient steepens above a magnitude threshold 70% and then becomes shallower above 80% apart from for configurations with size filter=1500. Since the median (Fig. S1d) can only take integer values, its behaviour is less consistent. Most of the lines still decrease with threshold, but the size filter 750 lines initially increase before decreasing again. Furthermore, while on the other plots, larger direction thresholds almost always lead to increases, increasing the direction filter often lead to decreases in the median length, showing that the days removed by these changes were usually part of longer events.

The patterns show that the increase in sensitivity of days per month to magnitude threshold above 70% (Fig. S1a) is due to days in long events being filtered out, leading to a reduction in the typical length of events (Fig. S1c). Increasing the magnitude threshold above 80% favours the exclusion of days in shorter events more strongly than in longer events, resulting in a sharper decrease in the typical number of events (Fig. S1b) but a stabilisation of the typical length (Fig. S1c).

To quantify the sensitivity, we have calculated the response of each statistic to 10% increase in each variable, while holding the other variables constant. To do this we have performed a linear regression of the percentage change of each statistic along each of the different parameter values, using parameter values as percentage changes relative to magnitude threshold=70%, direction threshold=45°, size threshold=1000. We have used these slopes to calculate the percentage change of the statistic under a 10% change in the parameter value. We display these as box plots in Fig. S2. Each point in the box plot is the sensitivity using the gradient with a certain combination of the other parameters. For example, each point in the magnitude threshold boxplot is the gradient of one of the lines in Fig. S1, which have constant values of direction and size. We then did the same for the other parameters.

Figures S2a–b show that, consistent with Fig. S1, both the total WMTE days per month and event count per month were most sensitive to magnitude threshold: a 10% increase in the magnitude threshold decreased the statistics by around 26–28%, while a 10% increase in direction or size filter resulted in only around a 3–5% increase or a 2.5% decrease respectively in the value of either of the statistics. Mean duration (Fig. S2c) was less sensitive: a 10% increase in size had almost no effect, and the 10% increase in magnitude lead to around a 7% decrease in mean duration. The effect of increasing the direction 10% was just above 0 for most parameter sets, but a few combinations reduced the mean duration, reflecting the possibility of adding short events to the set. Similar but

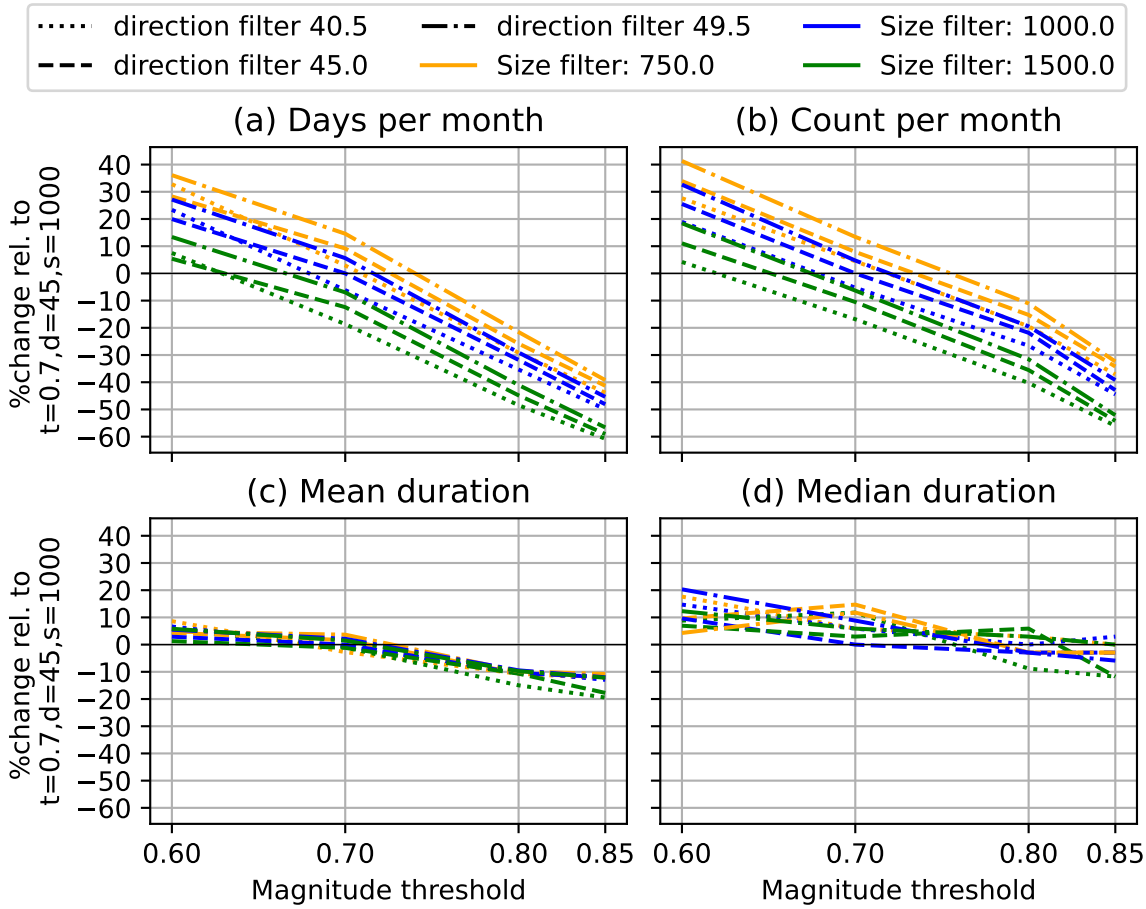

Figure S1: Statistics of WMTEs crossing the EEA line for different parameter combinations. The y axis shows the percentage change relative to the run with direction= 45°, size=1000 pixels, magnitude threshold=70%. **(a)** number of WMTE days per month, **(b)** count of WMTEs per month, **(c)** mean duration of WMTEs, **(d)** median duration of WMTEs.

more exaggerated patterns were observed in the median duration (Fig. S2d), where sensitivity to direction and size was again very small but the direction was split almost evenly. Increases in the magnitude threshold still caused a decrease, of about 5–6%.

Due to the extremely low sensitivity of the method to size threshold, we settled on a value of 1000 grid points because it was a convenient number that excluded the smallest areas of westerly transport that are less interesting. The model is slightly more sensitive to the direction, but given even in the peak WMTE season of JF, there were only around 10 days per year with a WMTE in EEA, the sensitivity of a few percent is relatively small. We settled on 45° since it is easy to argue that we are interested in vectors within 45° of due west when investigating westerly events.

Clearly, the choice of magnitude threshold is the most important. 70% is lower than the typical atmospheric river threshold, but since EEA is often affected by strong easterlies, we didn't want to exclude westerly days of reasonable magnitude from locations with high magnitude easterly transport. We opted for 70% because it is still high enough to exclude days with only weak westerly transport, but is more generous than the AR threshold, and in particular allowed us to capture long duration events (Fig. S1c) that may be important for allowing moisture to travel into EEA from the Congo basin.

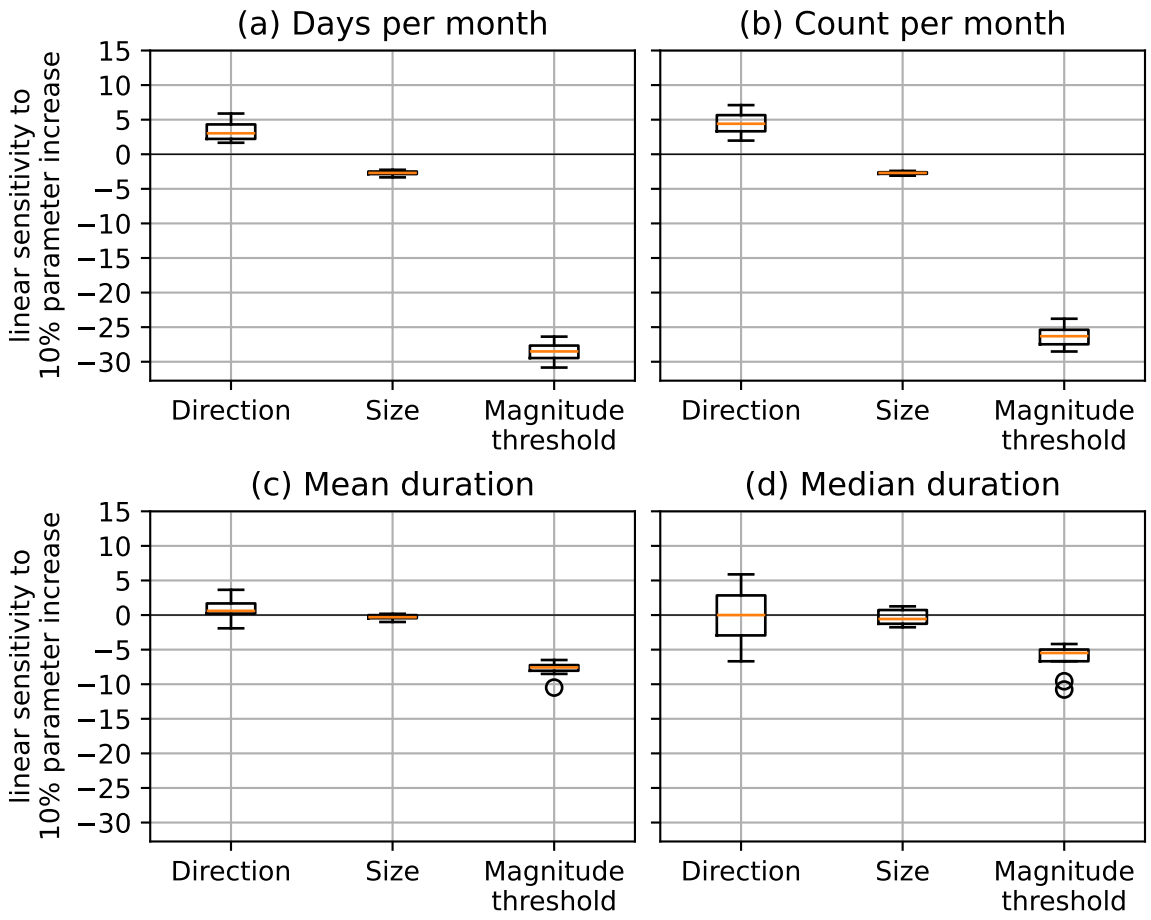

Figure S2: Sensitivity of statistics of WMTEs crossing the EEA line to a 10% parameter increase, when the other two parameters are held constant. Each datapoint contributing to the box plots represents one unique combination of the other two parameters. **(a)** the change in number of WMTE days per month when direction/size/threshold change by 10%, **(b)** same for count of WMTEs per month, **(c)** same for mean duration of WMTEs, **(d)** same for median duration of WMTEs. Points beyond the end of the whiskers are plotted.

S2 Risk ratio of WMTE occurrence in all seasons

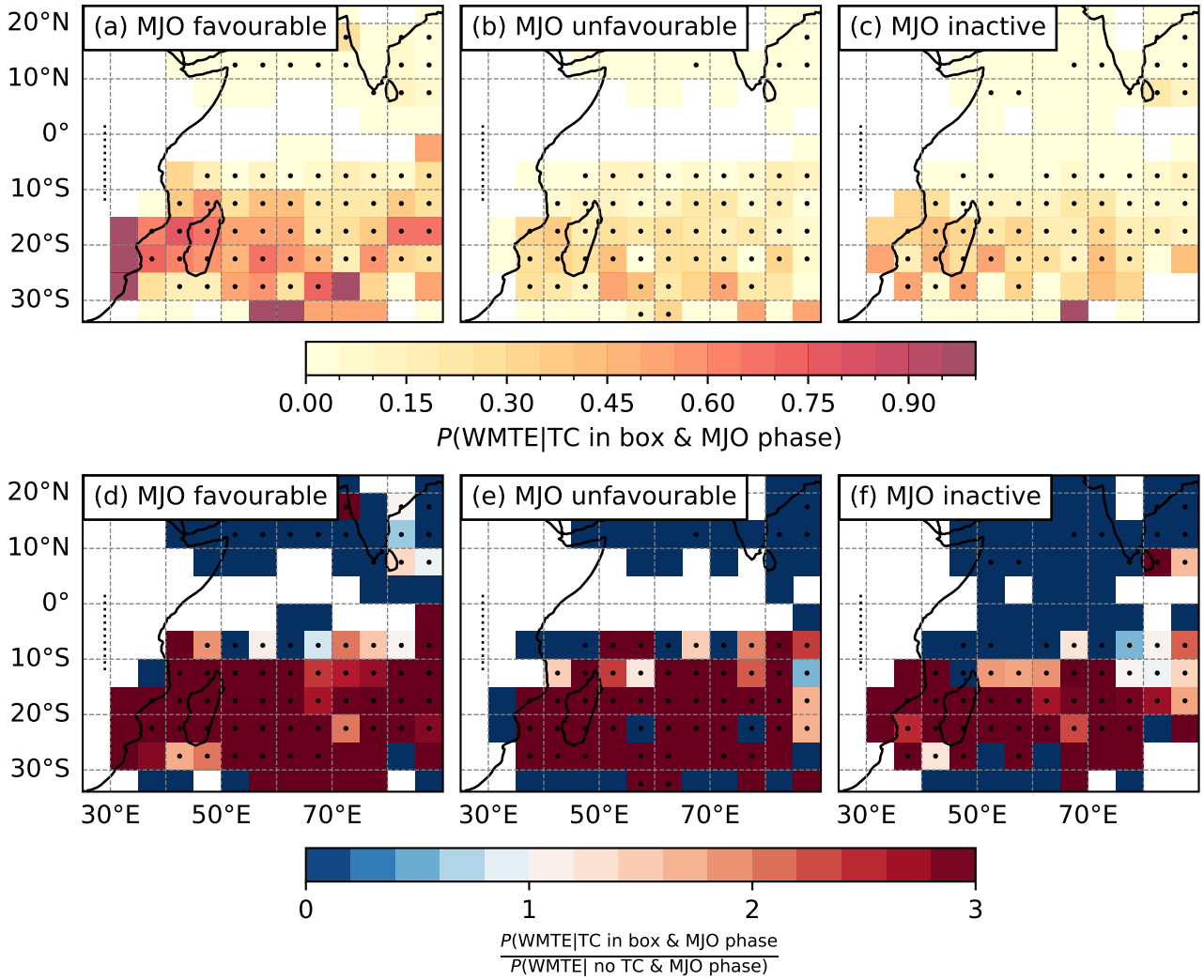

Figure S3: As Fig. 5 in main text, but the lower panels show all seasons. How the presence of a tropical cyclone at different locations changes the probability of a WMTE day in EEA. **(a–c)** The probability of a WMTE crossing the line at 29°E from 2°N to 12°S, shown by the black dashed line, given the presence of a TC in 5° grid boxes. **(d–f)** Relative risk for each box, showing the ratio of the probability of a WMTE crossing the line given the presence of a TC, compared to the probability of a WMTE crossing the line, given there is no TC anywhere in the Indian Ocean. Boxes with a dot have at least 5 TC reports in the period 1980–2022. **(a, d)** MJO phases 2–4, **(b, e)** MJO phases 5–1, **(c, f)** MJO inactive.

S3 Risk ratio for TC-WMTEs

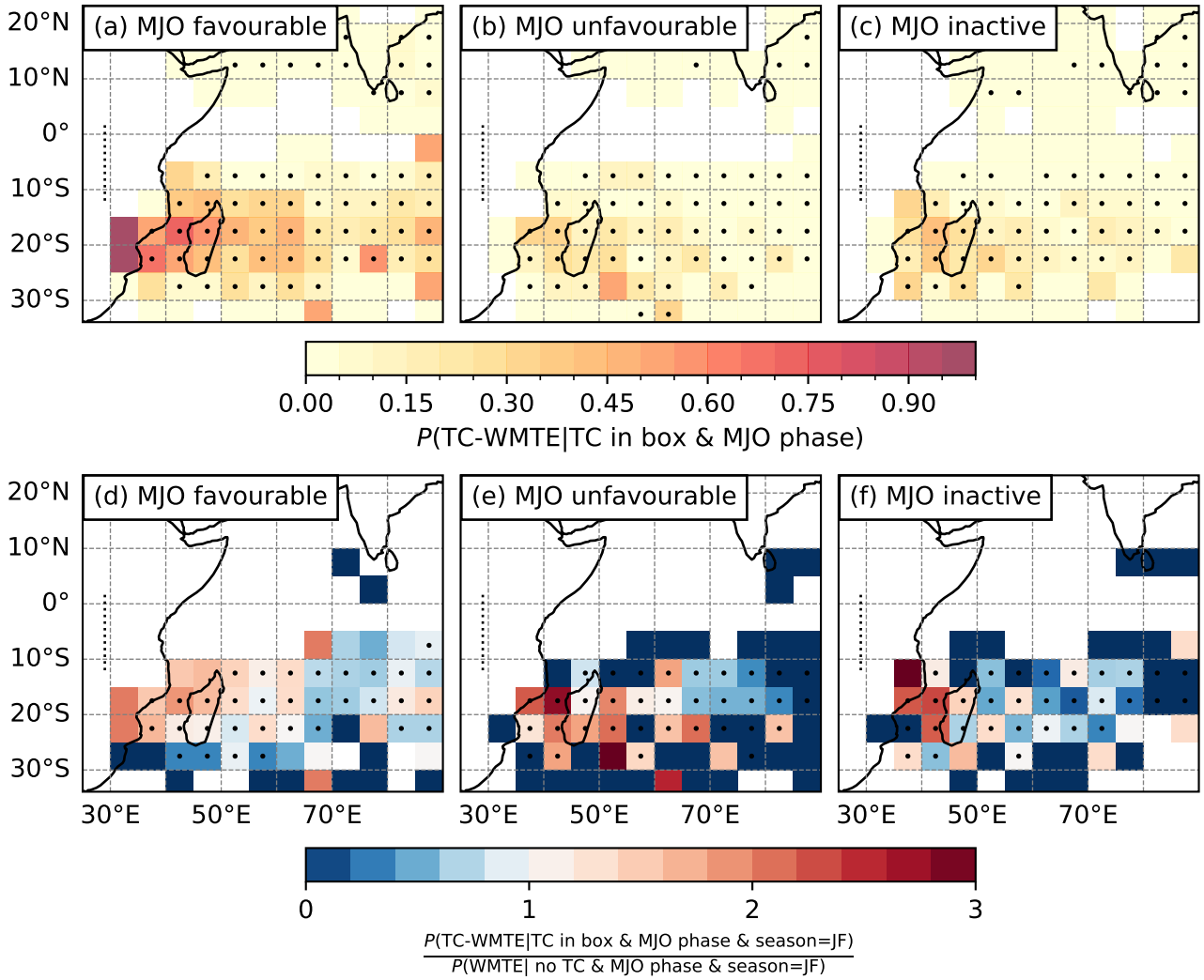

Figure S4: As Fig. 5 in main text, but with TC-WMTEs. How the presence of a tropical cyclone at different locations changes the probability of a TC-WMTE day in EEA. **(a–c)** The probability of a TC-WMTE crossing the line at 29°E from 2°N to 12°S, shown by the black dashed line, given the presence of a TC in 5° grid boxes. **(d–f)** JF relative risk for each box, showing the ratio of the probability of a TC-WMTE crossing the line given the presence of a TC, compared to the probability of a WMTE crossing the line, given there is no TC anywhere in the Indian Ocean. Boxes with a dot have at least 5 TC reports in the period 1980–2022. **(a, d)** MJO phases 2–4, **(b, e)** MJO phases 5–1, **(c, f)** MJO inactive.

S4 Precipitation dataset comparison

S4.1 ERA5 1998–2022

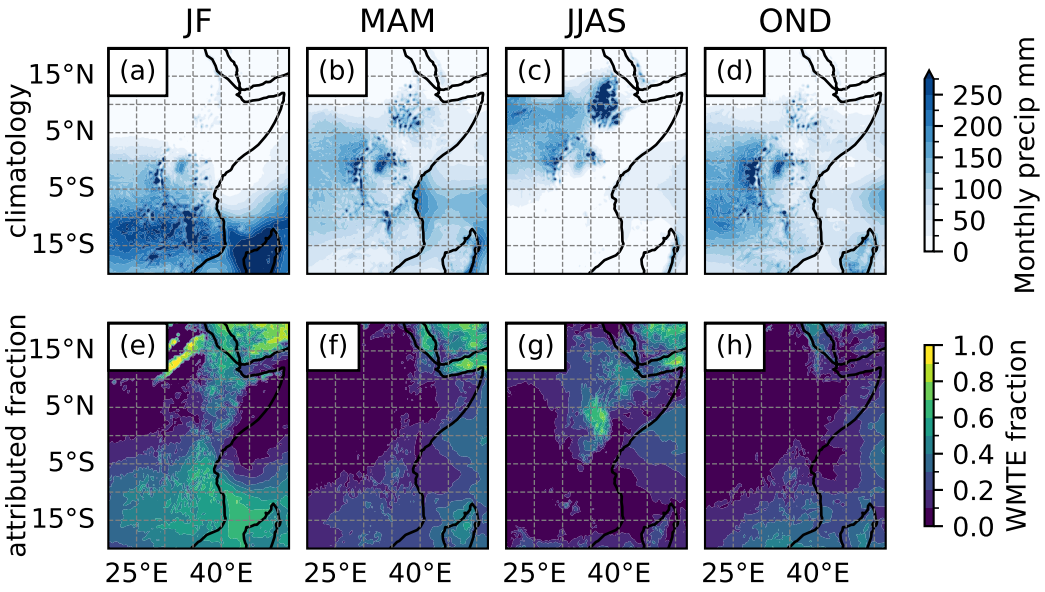

Figure S5: (a–d) The ERA5 average monthly precipitation from 1998 to 2022 in each season and (e–h) The fraction of precipitation that was attributed to WMTEs in each season

S4.2 CHIRPS 1998–2022

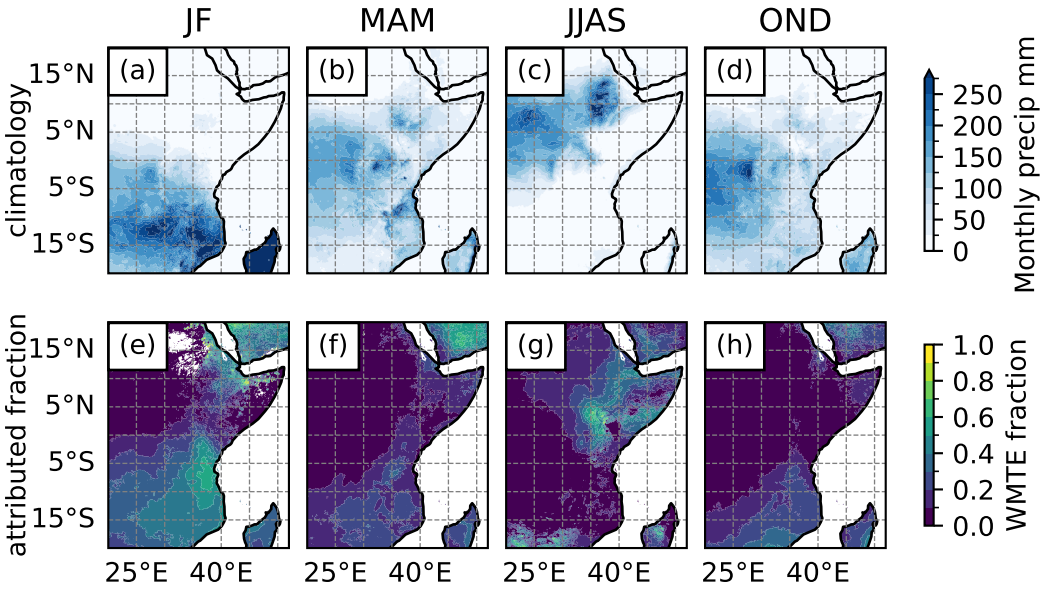

Figure S6: (a–d) The CHIRPS average monthly precipitation from 1998 to 2022 in each season and (e–h) The fraction of precipitation that was attributed to WMTEs in each season

S4.3 IMERG 1998–2022

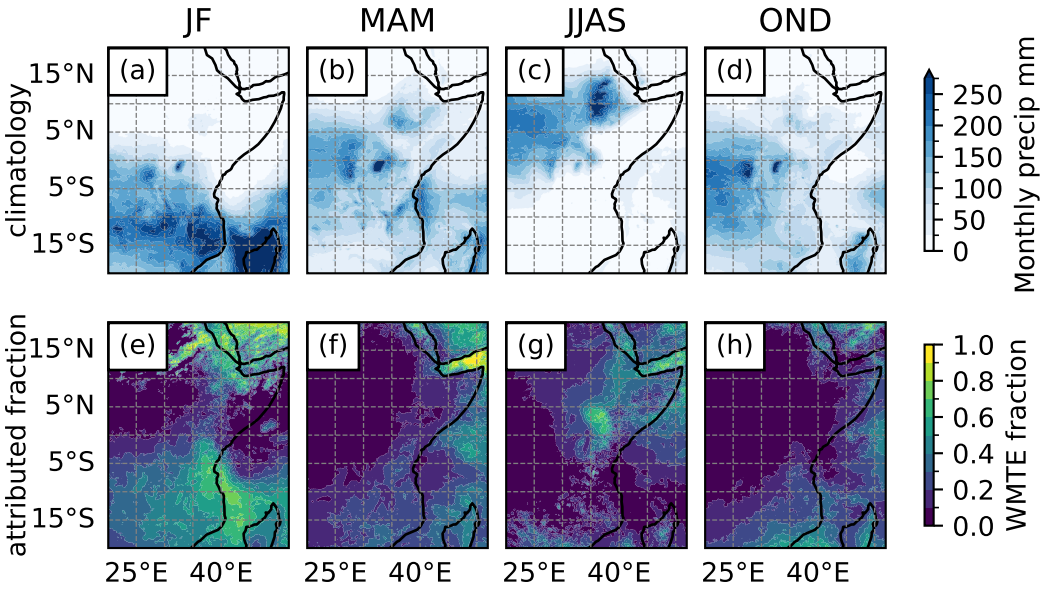

Figure S7: (a–d) The IMERG average monthly precipitation from 1998 to 2022 in each season and (e–h) The fraction of precipitation that was attributed to WMTEs in each season

References

Guan, Bin and Duane E. Waliser (2015). "Detection of atmospheric rivers: Evaluation and application of an algorithm for global studies". In: *Journal of Geophysical Research: Atmospheres* 120.24, pp. 12514–12535. DOI: https://doi.org/10.1002/2015JD024257.